ISSN 2075-1087, Gyroscopy and Navigation, 2024, Vol. 15, No.2, pp. 98-109.
Russian Text © The Author(s), 2024, published in Giroskopiya i Navigatsiya, 2024, No.2, pp. 151-167.

Deviation of Electromagnetic Pulses in Earth-Fixed Rotating Reference Frame

E. M. Mazurova[a, *], A. N. Petrov[a, b], F. S. Bakharev[a], and I. A. Klypin[a, c]

[a] [a]*Roskadastr Public Nonprofit Company, Moscow, Russia*
[b]*Sternberg Astronomical Institute (GAISh), Moscow State University, Moscow, Russia*
[c]*Moscow State University of Geodesy and Cartography (MIIGAiK), Moscow, Russia*

**e-mail*: *e_mazurova@mail.ru*
Received: December 27, 2023; reviewed: June 27, 2024; accepted: June 27, 2024

Abstract: The position of an Earth's space satellite (ESS) or the Moon is determined by laser ranging. The distances from the ground stations to satellites equipped with ranging reflectors or to the reflectors located on the Moon surface are measured by means of laser tools. Based on the time interval between the emission and reception of ultrashort laser pulses at the same station, it is possible to determine the position of an ESS or the Moon at the moment of reflection. In this case, the signal emitted from the station and the signal reflected from the satellite propagate along different paths. As a result, an angle between the directions of the emitted and returned signal is formed at the location point. It is this deviation of laser signal paths that is the subject matter of this paper. Since the Earth-fixed rotating reference frame is noninertial, calculations are performed with consideration for the theory of relativity. The spherical shape of the Earth and the Keplerian orbits of the ESS are considered without taking into account the Earth's gravity field. The signal deviation significantly depends both on the satellite orbital parameters and the Earth's rotation rate. The mathematical calculations allow the authors to generalize and compare the results of studies of this effect, obtained by other authors. They have also been used in the numerical calculations in a case study of a high-orbit and high-eccentricity satellite RadioAstron and all of the 24 GLONASS low-orbit satellites with minor eccentricities. The magnitudes of the effect and its variations depending on the changes in the satellite orbit parameters are calculated. The accuracy of modern instruments is sufficient to record the effect, and the result obtained will increase the efficiency of their application. In the future, it is planned to evaluate the factors of the Earth oblateness and its gravitational potential.

Keywords: Earth's space satellite, laser ranging.

1. INTRODUCTION

For decades, the relativistic effects (of the general relativity (GR) and special relativity (SR)) have been taken into account in calculating the motion of celestial bodies and the propagation of electromagnetic pulses. One of the examples taken from numerous publications is the case study [1], where the results considering the relativistic corrections were used in processing the trajectory measurements of a spacecraft launched to the Phobos, a satellite of the Mars, in 1988–1989. This significantly improved the accuracy of measurements even with the equipment of that time. A classical manual for calculating the trajectories of celestial bodies and the paths of electromagnetic pulses, taking into account the relativistic corrections, is the book by Brumberg [2].

The position of ESS or the Moon is determined mainly by the laser ranging method. Laser measurements of the distance are taken from ground stations to satellites equipped with ranging reflectors, or to the reflectors located on the Moon surface. Using the time interval between the emission and reception of ultrashort laser pulses at the same station, the position of the ESS or the Moon at the time of reflection is determined. According to recent articles [3–9], the intensity of these studies is extremely high.

The accuracy of the devices used in laser raging has increased significantly in our time. A growing part of the corrections occurring within the GR applications become available for measurement. These corrections need to be taken into account when operating the ESS for different purposes, as well as the navigation satellite systems [10]. Their functioning relies to a great extent upon the laser ranging of the ESS and the laser signals exchange between them. However, the mathematical models of signals' exchange between the ESS and the laser stations located on the Earth surface often neglect the Earth rotation, i.e., it is assumed implicitly that the reference frames of the stations are inertial.

In fact, the reference frames of laser stations are noninertial, since they are located on the rotating Earth. According to the equivalence principle underlying the GR, centrifugal potentials can be considered as gravitational ones, under the influence of which the light rays do bend. As a result, at the location point of the laser station, an angle is formed between the directions of the emitted signal and the signal reflected from the ESS. The effect of deflection of electromagnetic pulses is small, but it can be measured: according to [10], a deflection angle of up to 0.5 arc sec can be detected. The present work is devoted to the study of this effect. Due to the above reasons, the GR equations will be used for signal propagation simulation.

Optical effects in the reference frame of the rotating Earth are considered in many works [11–17]. The main focus is made on the deviation effect, but other important effects are also discussed, such as signals delay due to the ray path bending [14], the effect of shifting the center of the reflected pulse spot on the Earth's surface relative to the laser station itself, due to which the intensity of the returned pulse at the station location may be so weak that it would be difficult to detect [16, 17]; as well as the influence of the Earth's gravity field potential [12].

In this paper, theoretical calculations are performed in the topocentric reference frame of a laser station for the spherical shape of the Earth and the Keplerian orbits of the ESS, with the gravity field of the Earth being neglected. In this case, the designations t_1, t_2 and t_3 introduced in [1] are used for the time points of the signal emission, its reflection from the ESS and return to the laser station, respectively. Our mathematical calculations allow us to summarize the calculations from [13] and [15] and compare them to each other. In the future, it is planned to take into account some weaker factors such as the Earth's gravity field, compare the results to those from [12], and in addition, take into account the ellipticity of the Earth.

The main objective of the study is to determine the deviation of laser beams using the examples of various real-world ESS. To this end, proprietary computational algorithms have been developed for the approaches described in [13] and [15]. The magnitude of the effect has been calculated for the ESS RadioAstron [11] and for all 24 ESS of the GLONASS constellation [19]. The resulting values for the ESS of GLONASS-1 and GLONASS-23 are presented in the text of this article. The data for other GLONASS satellites differ from them insignificantly, so they are not given here.

In addition, variations of the effect were found for the ESS of the RadioAstron and the GLONASS-1 and GLONASS-23 with different parameters. In our opinion, such complete and detailed calculations have not been done before. In the future, after the appropriate theory has been developed, it is planned to adapt the algorithms to take into account the influence of weaker factors, and to compare the calculation results to the current ones.

2. TOPOCENTRIC CARTESIAN REFERENCE SYSTEM

The geocentric (equatorial) reference system (GRS) is one of the most important reference frames. Its origin is in the center of the Earth; it does not rotate, the x-axis is directed to the point of the vernal equinox at the equator, the y-axis is perpendicular to the x-axis at the equator, and the z-axis is perpendicular to the equatorial plane in the direction of the North Pole. Due to the limitations of our ideal model, where there are no gravitational potentials, it is convenient to choose the Minkowski metric for the GRS: $ds^2 = c^2dt^2 - dx^2 - dy^2 - dz^2$, where c is the speed of light, $ct = x^0$ is the time coordinate, and x, y, z are the spatial coordinates. The reference system of a local observer on the Earth's surface is called topocentric one; in our case it is an observer at a laser ranging station. The origin of this system with the coordinates x_s, y_s, z_s is matched with the location of this station, and the time is the same as in the GRS. The subscript "s" (station) emphasizes that it is exactly the reference system of the station. The axis x_s is directed along the meridian towards the equator (in the northern hemisphere), the axis y_s is directed along the parallel, and the axis z_s is directed to the zenith.

Let us consider a way to transit from one reference system to another. If both of them are Cartesian, then the simplest option is appropriate rotations relative to a certain axis. To convert the GRS coordinates to topocentric ones, we first transit to a rotating reference system, according to [20]. Then the origin is transferred to the station location point with longitude λ_0 and latitude φ_0, after which the axes are rotated in accordance with the definition of a topocentric reference system given above. As a result, the metric of the Minkowski space in the GRS with coordinates (x, y, z) will take the following form in the topocentric coordinates (x_s, y_s, z_s):

$$ds_s^2 = \left[1 - \frac{\Omega^2}{c^2}\left(\left[x_s \sin\varphi_0 + (z_s + R_\oplus)\cos\varphi_0\right]^2 + y_s^2\right)\right]c^2 dt^2$$
$$+2y_s \sin\varphi_0 \frac{\Omega}{c} dx_s c dt - 2\left[x_s \sin\varphi_0 + (z_s + R_\oplus)\cos\varphi_0\right]\frac{\Omega}{c} dy_s c dt$$
$$+2y_s \cos\varphi_0 \frac{\Omega}{c} dz_s c dt - dx_s^2 - dy_s^2 - dz_s^2. \quad (1)$$

It is in topocentric coordinates that we will write down the equations for both the ESS motion and the propagation of laser pulses.

3. ESS COORDINATES IN TOPOCENTRIC COORDINATE SYSTEM

We determine the coordinates of satellite in the topocentric coordinate system according to [21]. First, we consider the ESS motion in the plane of the orbit with the following main characteristics: a is the semimajor axis, and e is the eccentricity. Axis $\boldsymbol{x}'$ is directed from the center to the perigee, axis $\boldsymbol{y}'$ is perpendicular to it in the orbit plane, and axis z' is perpendicular to the orbit plane. The angle v between the direction to the ESS and axis $\boldsymbol{x}'$ is called the true anomaly, and the auxiliary angle E is called the eccentric anomaly. The coordinates of the ESS moving in orbit and the radial distance from the center of the Earth to this ESS can be represented as

$$x' = r\cos\nu = a(\cos E - e),$$
$$y' = r\sin\nu = a\sqrt{1-e^2}\sin E, \quad (2)$$
$$r = \sqrt{x'^2 + y'^2} = a(1 - e\cos E).$$

The eccentric anomaly changes over time t in accordance with the Kepler equation:

$$E(t) - e\sin E(t) = \sqrt{GM_\oplus / a^3}\,(t - t_p), \quad (3)$$

where G and $M_\oplus$ are the gravitational constant and the mass of the Earth; t_p is the time of perigee passage.

The parameters of the orbit relative to the equatorial plane are as follows: i is the angle of the orbit plane inclination relative to the equatorial plane; ω is the angle between the node line and the direction to the perigee in the orbit plane (the perigee argument); λ is the angle between the direction to the vernal equinox point and the node line in the equatorial plane.

To move from describing the ESS motion in the plane of its orbit in coordinates (x′, y') to describing it in topocentric coordinates (x_s, y_s, z_s), it is necessary to first transit to the GRS. To do so, we make a turn at an angle ω in orbit plane for (2), matching the direction to the perigee and the orbit node line, and then make a turn around this line at an angle i, matching the planes of the orbit and the equator. Finally, we make a turn at an angle λ in the equatorial plane, matching the node line and the direction to the vernal equinox point. As a result, we obtain the coordinates of the ESS in the GRS.

To transit to the topocentric coordinate system, the above rotations are performed first around the z-axis at an angle Ωt, assuming that at the time t = 0 the Greenwich meridian coincides with the direction to the vernal equinox point. We obtain a rotating system in which the distance from the center of the Earth to the ESS is determined. Then the origin is moved from the center of the Earth to the location of the station at a distance of the Earth's radius $R_\oplus$ and the radius vector from the station to the ESS is calculated. By contracting this expression with unitary orthonormal vectors of the topocentric coordinate system, we find the coordinates of the ESS in the topocentric coordinate system:

$$x_s = a\left\{\left[\cos\omega\cos(\Omega t + \lambda_0 - \lambda) + \sin\omega\cos i\sin(\Omega t + \lambda_0 - \lambda)\right]\sin\varphi_0 - \sin\omega\sin i\cos\varphi_0\right\}(\cos E - e) -$$
$$-a\sqrt{1-e^2}\left\{\left[\sin\omega\cos(\Omega t + \lambda_0 - \lambda) - \cos\omega\cos i\sin(\Omega t + \lambda_0 - \lambda)\right]\sin\varphi_0 + \cos\omega\sin i\cos\varphi_0\right\}\sin E, \quad (4a)$$

$$y_s = a\left[-\cos\omega\sin(\Omega t + \lambda_0 - \lambda) + \sin\omega\cos i\cos(\Omega t + \lambda_0 - \lambda)\right](\cos E - e) +$$
$$+a\sqrt{1-e^2}\left[\sin\omega\sin(\Omega t + \lambda_0 - \lambda) + \cos\omega\cos i\cos(\Omega t + \lambda_0 - \lambda)\right]\sin E, \quad (4b)$$

$$z_s = a\left\{\left[\cos\omega\cos(\Omega t + \lambda_0 - \lambda) + \sin\omega\cos i\sin(\Omega t + \lambda_0 - \lambda)\right]\cos\varphi_0 + \sin\omega\sin i\sin\varphi_0\right\}(\cos E - e) -$$
$$-a\sqrt{1-e^2}\left\{\left[\sin\omega\cos(\Omega t + \lambda_0 - \lambda) - \cos\omega\cos i\sin(\Omega t + \lambda_0 - \lambda)\right]\cos\varphi_0 - \cos\omega\sin i\sin\varphi_0\right\}\sin E - R_\oplus. \quad (4c)$$

4. EQUATIONS OF LIGHT GEODESICS[1] IN TOPOCENTRIC COORDINATE SYSTEM

To form the equations of light beams propagation in a topocentric reference frame, we use metric (1) and the GR equations written for it. For zero-mass particles, the equation of the geodesic has the form $dk^\alpha/d\sigma + \Gamma^\alpha_{\mu\nu}k^\mu k^\nu = 0$. Here, $k^\alpha = dx^\alpha/d\sigma = (x^\alpha)'$ is the vector tangent to the global light-like line, and σ is an arbitrary parameter along this line. Greek indices α specify the space-time coordinates $x^\alpha = (x^0, x^1, x^2, x^3)$, Latin indices i specify the spatial coordinates $x^i = (x^1, x^2, x^3) = (x_s, y_s, z_s)$, and $\Gamma^\alpha_{\mu\nu}$ are the Christoffel symbols.

For metric (1), $\Gamma^0_{\mu\nu} = 0$, so the zero component in the equation of the geodesic has the form $(x^0)'' = 0$, the simplest solution to which is $x^0 = \sigma$. Therefore, for the remaining three components of the equation of the geodesic, parameter σ can be replaced with a time coordinate x^0, and the GR equation can be presented in the form:

$$\begin{aligned}
&\ddot{x}_s - 2\frac{\Omega}{c}\dot{y}_s\sin\varphi_0 - \frac{\Omega^2}{c^2}\left[x_s\sin\varphi_0 + (z_s + R_\oplus)\cos\varphi_0\right]\sin\varphi_0 = 0,\\
&\ddot{y}_s + 2\frac{\Omega}{c}\dot{x}_s\sin\varphi_0 + 2\frac{\Omega}{c}\dot{z}_s\cos\varphi_0 - \frac{\Omega^2}{c^2}y_s = 0,\\
&\ddot{z}_s - 2\frac{\Omega}{c}\dot{y}_s\cos\varphi_0 - \frac{\Omega^2}{c^2}\left[x_s\sin\varphi_0 + (z_s + R_\oplus)\cos\varphi_0\right]\cos\varphi_0 = 0,
\end{aligned} \tag{5}$$

where the dot above symbols marks differentiation with respect to x_0. The relationship for the light-like geodesic line $k^\alpha k_\alpha = g_{\alpha\beta}k^\alpha k^\beta = 0$ yields

$$\begin{aligned}
&\dot{x}_s^2 + \dot{y}_s^2 + \dot{z}_s^2 =\\
&= 1 - \frac{\Omega^2}{c^2}\left(\left[x_s\sin\varphi_0 + (z_s + R_\oplus)\cos\varphi_0\right]^2 + y_s^2\right) +\\
&+2\frac{\Omega}{c}\dot{x}_s y_s\sin\varphi_0 + 2\frac{\Omega}{c}\dot{z}_s y_s\cos\varphi_0 -\\
&-2\frac{\Omega}{c}\dot{y}_s\left[x_s\sin\varphi_0 + (z_s + R_\oplus)\cos\varphi_0\right].
\end{aligned} \tag{6}$$

Set of equations (5) has a solution in the topocentric coordinates:

$$\begin{aligned}
&x_s(t) =\\
&= \left[\left(A + Mx^0\right)\cos\left(\Omega t + \lambda_0\right) + \left(B + Nx^0\right)\sin\left(\Omega t + \lambda_0\right)\right]\sin\varphi_0 -\\
&-\left(C + Kx^0\right)\cos\varphi_0,
\end{aligned} \tag{7a}$$

$$\begin{aligned}
&y_s(t) =\\
&= -\left(A + Mx^0\right)\sin\left(\Omega t + \lambda_0\right) + \left(B + Nx^0\right)\cos\left(\Omega t + \lambda_0\right),
\end{aligned} \tag{7b}$$

$$\begin{aligned}
&z_s(t) =\\
&= \left[\left(A + Mx^0\right)\cos\left(\Omega t + \lambda_0\right) + \left(B + Nx^0\right)\sin\left(\Omega t + \lambda_0\right)\right]\cos\varphi_0 +\\
&+\left(C + Kx^0\right)\sin\varphi_0 - R_\oplus.
\end{aligned} \tag{7c}$$

Values *A, B, C* and *M, N, K* are the integration constants. Based on (6), we write the relationship $M^2 + N^2 + K^2 = 1$. The solution of (7) is general and is used for describing the paths of laser pulses propagation to and from the ESS.

5. VECTORS TANGENT TO THE PATH OF EMITTED PULSE

Taking into account the fact that at the moment of emission t_1 the coordinates in the left part of equations (7) are equal to zero, *A, B, C* are determined through *M, N, K* and substituted in (7). At the moment t_2 when the pulse reaches the ESS, the coordinates of the former $x_{out}(t)$, $y_{out}(t)$, $z_{out}(t)$ in (7) coincide with the coordinates of the latter in (3):

$$\begin{aligned}
&x_s\left(E(t_2), t_2\right) = x_{out}(t_2),\ y_s\left(E(t_2), t_2\right) = y_{out}(t_2),\\
&z_s\left(E(t_2), t_2\right) = z_{out}(t_2).
\end{aligned} \tag{8}$$

As we can remember, $E(t)$ is defined in (2). Then the values of the ESS coordinates (4) as of the moment of contact with the pulse are fixed:

$$\begin{aligned}
&x_S \equiv x_s\left(E(t_2), t_2\right),\ y_S \equiv y_s\left(E(t_2), t_2\right),\\
&z_S \equiv z_s\left(E(t_2), t_2\right),
\end{aligned} \tag{9}$$

after which the constants *M, N, K* are calculated using x_S, y_S, z_S. Hereinafter, the notation $E(t_2) = E_2$ will be used. Substitution of *M, N, K* in $M^2 + N^2 + K^2 = 1$ gives a useful relationship:

[1] The geodesic is usually understood as a global line (a curve in 4D space-time) showing the motion of a point particle, or a test high-mass particle or a zero-mass particle, e.g., a photon (laser pulse) [20]. The equation of the geodesic has 4 components. The geodesic of a photon is called light, light-like, or isotropic, or zero geodesic.

$$c^2\left[t_p+\sqrt{a^3/GM_\oplus}\,(E_2-e\sin E_2)-t_1\right]^2=R_\oplus^2+a^2\left[1-e\cos E_2\right]^2-2aR_\oplus\{\sin\varphi_0\sin i\sin\omega+$$
$$+\cos\varphi_0\left[\cos\omega\cos(\Omega t_1+\lambda_0-\lambda)+\cos i\sin\omega\sin(\Omega t_1+\lambda_0-\lambda)\right]\}\times(\cos E_2-e)-2aR_\oplus\sqrt{1-e^2}\,\{\sin\varphi_0\sin i\cos\omega- \quad (10)$$
$$-\cos\varphi_0\left[\sin\omega\cos(\Omega t_1+\lambda_0-\lambda)-\cos i\cos\omega\sin(\Omega t_1+\lambda_0-\lambda)\right]\}\sin E_2.$$

Substitution of calculated M, N, K in (7) defines the functions for the emitted signals $x_{out}(t, x_S, y_S, z_S)$, $y_{out}(t, x_S, y_S, z_S)$ and $z_{out}(t, x_S, y_S, z_S)$. Their differentiation with respect to x^0 and selection of the values of derivatives at the moment t_1 provides the components of the vector tangent to the emitted signal path:

$$\boldsymbol{k}_1=\boldsymbol{k}_1((t_2-t_1),x_S,y_S,z_S)=\left[k_1^1,k_1^2,k_1^3\right], \quad (11)$$

the components of which are described in [13] and have the form:

$$k_1^1=\left.\frac{dx_{out}(t)}{dx^0}\right|_{t=t_1}=$$
$$=\frac{1}{c(t_2-t_1)}\{x_S\left[\cos\Omega(t_2-t_1)\sin^2\varphi_0+\cos^2\varphi_0\right]-y_S\sin\Omega(t_2-t_1)\sin\varphi_0+(z_S+R_\oplus)\left[\cos\Omega(t_2-t_1)-1\right]\cos\varphi_0\sin\varphi_0\}, \quad (12a)$$

$$k_1^2=\left.\frac{dy_{out}(t)}{dx^0}\right|_{t=t_1}=\frac{1}{c(t_2-t_1)}\{x_S\sin\Omega(t_2-t_1)\sin\varphi_0+y_S\cos\Omega(t_2-t_1)+(z_S+R_\oplus)\sin\Omega(t_2-t_1)\cos\varphi_0\}-\frac{\Omega}{c}R_\oplus\cos\varphi_0, \quad (12b)$$

$$k_1^3=\left.\frac{dz_{out}(t)}{dx^0}\right|_{t=t_1}=$$
$$=\frac{1}{c(t_2-t_1)}\{x_S\left[\cos\Omega(t_2-t_1)-1\right]\cos\varphi_0\sin\varphi_0-y_S\sin\Omega(t_2-t_1)\cos\varphi_0+(z_S+R_\oplus)\left[\cos\Omega(t_2-t_1)-1\right]\cos^2\varphi_0+z_S\}. \quad (12c)$$

To obtain the formulae presented in [15], we substitute (9) which incorporate the equations (7) in (12) and obtain

$$k_1^1=\frac{a(\cos E_2-e)}{c(t_2-t_1)}\{\left[\cos\omega\cos(\Omega t_1+\lambda_0-\lambda)+\sin\omega\cos i\sin(\Omega t_1+\lambda_0-\lambda)\right]\times\sin\varphi_0-\sin\omega\sin i\cos\varphi_0\}-$$
$$-\frac{a\sqrt{1-e^2}\sin E_2}{c(t_2-t_1)}\{\left[\sin\omega\cos(\Omega t_1+\lambda_0-\lambda)-\cos\omega\cos i\sin(\Omega t_1+\lambda_0-\lambda)\right]\sin\varphi_0+\cos\omega\sin i\cos\varphi_0\}, \quad (13a)$$

$$k_1^2=\frac{a(\cos E_2-e)}{c(t_2-t_1)}\left[-\cos\omega\sin(\Omega t_1+\lambda_0-\lambda)+\sin\omega\cos i\cos(\Omega t_1+\lambda_0-\lambda)\right]+$$
$$+\frac{a\sqrt{1-e^2}\sin E_2}{c(t_2-t_1)}\left[\sin\omega\sin(\Omega t_1+\lambda_0-\lambda)+\cos\omega\cos i\cos(\Omega t_1+\lambda_0-\lambda)\right]-\frac{\Omega R_\oplus}{c}\cos\varphi_0, \quad (13b)$$

$$k_1^3=\frac{a(\cos E_2-e)}{c(t_2-t_1)}\{\left[\cos\omega\cos(\Omega t_1+\lambda_0-\lambda)+\sin\omega\cos i\sin(\Omega t_1+\lambda_0-\lambda)\right]\times\cos\varphi_0+\sin\omega\sin i\sin\varphi_0\}-$$
$$-\frac{a\sqrt{1-e^2}\sin E_2}{c(t_2-t_1)}\{\left[\sin\omega\cos(\Omega t_1+\lambda_0-\lambda)-\cos\omega\cos i\sin(\Omega t_1+\lambda_0-\lambda)\right]\cos\varphi_0-\cos\omega\sin i\sin\varphi_0\}-\frac{R_\oplus}{c(t_2-t_1)}. \quad (13c)$$

6. VECTORS TANGENT TO THE PATH OF RETURNED PULSE

In this case, the procedure is the same as in the previous section. At first, integration constants are calculated with reference to the moment of reflection t_2 and the moment of reception t_3. Then the relationship similar to (10) is defined:

$$c^2\left[t_3 - t_p - \sqrt{a^3/GM_\oplus}\left(E_2 - e\sin E_2\right)\right]^2 = R_\oplus^2 + a^2\left[1 - e\cos E_2\right]^2 - 2aR_\oplus\left\{\sin\varphi_0\sin i\sin\omega + \right.$$
$$\left. + \cos\varphi_0\left[\cos\omega\cos(\Omega t_3 + \lambda_0 - \lambda) + \cos i\sin\omega\sin(\Omega t_3 + \lambda_0 - \lambda)\right]\right\} \times \left(\cos E_2 - e\right) - 2aR_\oplus\sqrt{1-e^2}\left\{\sin\varphi_0\sin i\cos\omega\right.$$
$$\left. - \cos\varphi_0\left[\sin\omega\cos(\Omega t_3 + \lambda_0 - \lambda) - \cos i\cos\omega\sin(\Omega t_3 + \lambda_0 - \lambda)\right]\right\}\sin E_2.$$

After that, the components of the vector tangent to the path of returned signal are written with opposite sign:

$$\boldsymbol{k}_3 = \boldsymbol{k}_3((t_3 - t_2), x_S, y_S, z_S) = -\left[k_3^1, k_3^2, k_3^3\right], \quad (15)$$

the components of which are described in [13] and have the form:

$$k_3^1 = $$
$$= \frac{1}{c(t_3 - t_2)}\left\{-x_S\left[\cos\Omega(t_3 - t_2)\sin^2\varphi_0 + \cos^2\varphi_0\right] - y_S\sin\Omega(t_3 - t_2)\sin\varphi_0 - \left(z_S + R_\oplus\right)\left[\cos\Omega(t_3 - t_2) - 1\right]\cos\varphi_0\sin\varphi_0\right\}, \quad (16a)$$

$$k_3^2 = \frac{1}{c(t_3 - t_2)}\left\{x_S\sin\Omega(t_3 - t_2)\sin\varphi_0 - y_S\cos\Omega(t_3 - t_2) + \left(z_S + R_\oplus\right)\sin\Omega(t_3 - t_2)\cos\varphi_0\right\} - \frac{\Omega}{c}R_\oplus\cos\varphi_0, \quad (16b)$$

$$k_3^3 = $$
$$= \frac{1}{c(t_3 - t_2)}\left\{-x_S\left[\cos\Omega(t_3 - t_2) - 1\right]\cos\varphi_0\sin\varphi_0 - y_S\sin\Omega(t_3 - t_2)\cos\varphi_0 - \left(z_S + R_\oplus\right)\left[\cos\Omega(t_3 - t_2)\cos^2\varphi_0 + \sin^2\varphi_0\right] + R_\oplus\right\}. \quad (16c)$$

To obtain the relations presented in [15], we substitute (9) which incorporate the equations (7) in (16), so that

$$k_3^1 = \frac{a\left(\cos E_2 - e\right)}{c(t_3 - t_2)}\left\{\left[\cos\omega\cos(\Omega t_3 + \lambda_0 - \lambda) + \sin\omega\cos i\sin(\Omega t_3 + \lambda_0 - \lambda)\right]\times\sin\varphi_0 - \sin\omega\sin i\cos\varphi_0\right\} -$$
$$- \frac{a\sqrt{1-e^2}\sin E_2}{c(t_3 - t_2)}\left\{\left[\sin\omega\cos(\Omega t_1 + \lambda_0 - \lambda) - \cos\omega\cos i\sin(\Omega t_1 + \lambda_0 - \lambda)\right]\sin\varphi_0 + \cos\omega\sin i\cos\varphi_0\right\}, \quad (17a)$$

$$k_3^2 = + \frac{a\left(\cos E_2 - e\right)}{c(t_3 - t_2)}\left[-\cos\omega\sin(\Omega t_3 + \lambda_0 - \lambda) + \sin\omega\cos i\cos(\Omega t_3 + \lambda_0 - \lambda)\right] +$$
$$+ \frac{a\sqrt{1-e^2}\sin E_2}{c(t_3 - t_2)}\left[\sin\omega\sin(\Omega t_3 + \lambda_0 - \lambda) + \cos\omega\cos i\cos(\Omega t_3 + \lambda_0 - \lambda)\right] + \frac{\Omega R_\oplus}{c}\cos\varphi_0, \quad (17b)$$

$$k_3^3 = \frac{a\left(\cos E_2 - e\right)}{c(t_3 - t_2)}\left\{\left[\cos\omega\cos(\Omega t_3 + \lambda_0 - \lambda) + \sin\omega\cos i\sin(\Omega t_3 + \lambda_0 - \lambda)\right]\times\cos\varphi_0 + \sin\omega\sin i\sin\varphi_0\right\} +$$
$$+ \frac{a\sqrt{1-e^2}\sin E_2}{c(t_3 - t_2)}\left\{\left[-\sin\omega\cos(\Omega t_3 + \lambda_0 - \lambda) + \cos\omega\cos i\sin(\Omega t_3 + \lambda_0 - \lambda)\right]\cos\varphi + \cos\omega\sin i\sin\varphi_0\right\}\sin E_2 - \frac{R_\oplus}{c(t_3 - t_2)}. \quad (17c)$$

In real studies, it is important to choose a proper type of reflectors installed on the ESS [16, 17]. The above calculations are based on the fact that the coordinates of both the emitted pulse at the moment t_1, and for the reflected pulse at the moment t_3 have the values $x_s(t_1) = x_s(t_3) = 0$, $y_s(t_1) = y_s(t_3) = 0$ and $z_s(t_1) = z_s(t_3) = 0$ in (7), i.e., the pulse returns at the same point (the origin of the topocentric coordinate system). If the pulse is reflected along a beam the tangent to which at the reflection point coincides with the tangent to the beam along which this pulse arrived at the reflector, the reflected light pulse may fail to be captured by the receiving telescope because of the curvature of the light beams and a narrow directional pattern. For this reason, it is supposed (e.g., in [13]) to use a reflector with a wide directional pattern, such as a cataphot, which will ensure that part of the reflected pulse returns at the emission point.

7. ANGLE BETWEEN EMITTED AND RETURNED PULSES

All the formulae obtained above have been written out without approximations within the framework of an ideal model. It is difficult to identify the effect itself without approximations, but since the angle between the vectors k_1 and k_3 is very small (even its significant value turns out to be no more than $\alpha \sim 10^{-5}$ rad), it is enough to make the appropriate simplifications. First, we replace the $\sin\alpha$ function with its argument, and the exact formula with an approximate one:

$$\alpha = \left\{2\left[1 - \frac{\boldsymbol{k}_1 \cdot \boldsymbol{k}_3}{|\boldsymbol{k}_1||\boldsymbol{k}_3|}\right]\right\}^{1/2} = \frac{|\boldsymbol{k}_1 \times \boldsymbol{k}_3|}{|\boldsymbol{k}_1||\boldsymbol{k}_3|}. \qquad (18)$$

This value differs from the next term in the $\sin\alpha$ expansion by the value $\sim\alpha^3/3! \sim 10^{-16}$ rad, which is unobservable, and this makes it possible to use (18) as an exact formula. The angle can be calculated by this formula in two ways.

The first method involves formulae (12) for k_1 and (16) for k_3. This method corresponds to the method in [13]. The components (12) of the k_1 vector depend significantly on the difference $t_2 - t_1$, while the components (15) of the k_3 vector depend on $t_3 - t_2$. For orbits of satellites at a distance of tens of thousands kilometers, these time intervals satisfy the inequalities: $t_2 - t_1 < 2$ s and $t_3 - t_1 < 2$ s. They are included in (12) and (15) as multipliers to the angular velocity of the Earth's rotation $\Omega \approx 7\times10^{-5}$ rad $\times$ s^{-1}; therefore, the value δ is chosen as a small parameter for subsequent expansions, which has the order $\delta \approx \Omega(t_2 - t_1) \approx \Omega(t_3 - t_2)$ and satisfies the inequality $\delta < 2\times10^{-4}$. Substituting (12) and (15) into (18), taking into account approximations, gives

$$\alpha = \frac{2\Omega}{c}\sqrt{y_S^2 + (x_S \sin\varphi_0 + z_S \cos\varphi_0)^2}. \qquad (19)$$

The next order of approximations has a magnitude $\alpha\delta$ less than 2×10^{-9} rad for $\alpha \sim 10^{-5}$, i.e. less than thousandths of arc second, which is not observable yet. Moreover, the accuracy of the calculations itself does not exceed this value either. In addition, when deriving (19), multiplier $c(t_3 - t_1) / 2R_S$ was replaced with 1, and after applying the relations for t_1 and t_3 taken from [6] and the values of the entered parameters, has become equal to $\sim(1 \pm 2 \times 10^{-11})$. Thus, formula (19) for the model under consideration is quite illustrative and absolutely sufficient in terms of both observational capabilities and numerical calculation.

Let us use the following calculation procedure. First, we assume that the time t_p spent by the ESS in the perigee has some value, and its change determines only the displacement of the curves along the time axis. This is not very important, since calculations are made for the entire orbital period. Second, the value of the eccentric anomaly E_2 at the point of the orbit where the reflection occurs is set. Then t_2 can be calculated using (3). By substituting the values of E_2 and t_2 in (4) we calculate x_S, y_S, z_S, and by substituting the latter in (19) the magnitude of the pulse deviation is calculated.

Let us discuss some features of formula (19). Assume that relativistic effects are not taken into account. Then the simplest reasoning is as follows. A signal is sent from the station to a satellite located at a distance R_S from it. The time of the pulse trip to the satellite and back will be $t_3 - t_1 = 2R_S$/s. During this time, the station will move to a distance of $\Omega R_\oplus \cos\varphi_0(t_3 - t_1) = 2R_S\Omega R_\oplus \cos\varphi_0$/s, i.e. the angles for the emitted and returned signals should be different even in this simplest case, without taking into account the non-inertial type of the reference frame. In a linear approximation, their difference is defined by the ratio of the station displacement to the distance to the satellite, that is, $\alpha^0 = 2\Omega R_\oplus \cos\varphi_0$/s.

As one can see, the result does not depend on the satellite's orbit parameters. Are they taken into account in the initial formula (19)? Yes, they are. In order to check this, it is necessary to reset all the parameters of the orbit and recall the formula for z_S in (7c), where the term $R_\oplus$ (radius of the Earth) has a sense of a free parameter (not related to the orbit). Then formula (19) will give exactly this value

$\alpha^0 = 2\Omega R_\oplus \cos\varphi_0/s$. Certainly, in calculations, it is necessary to use a full formula (19) where all the effects are present. Nevertheless, we estimate the maximum contribution of α^0 when the station is located at the equator and the satellite's orbit lies in the equatorial plane. Then, for standard values of the Earth parameters, $\alpha^0 = 0.64''$.

According to the second method, we estimate the angle between vectors k_1 and k_3, which corresponds to the method from [15]. First, the transcendental equation (10) is numerically solved to determine E_2 as a function of the ESS orbit parameters, station location data and the time point t_1. Then the components of vector k_1 are found (see (13)). Similarly, using (14) and (17), the components of vector k_3 are found. The calculated values of k_1 and k_3 are substituted in (18).

Let us compare both methods. Calculation according to the method proposed in [6] involves an already approximated formula (19), while calculation according to the second method [15] is based on the exact formulae of both the transcendental equations (10) and (14) which are solved numerically, and the exact formulae (13) and (17). As was noted above, the accuracy of formula (19) in absolute terms is more than sufficient within the framework of modern measurement accuracy. Furthermore, the numerical calculation method also has an accuracy of up to thousandths of a second, i.e., the approximated formula (19) may be used as well. Finally, the results obtained by both methods also differ by no more than thousandths of a second. Thus, both methods can be applied, although the first one seems to be more efficient.

8. NUMERICAL CALCULATIONS FOR RADIOASTRON AND GLONASS ESS

As a rule, the authors of [6] and [15] used the RadioAstron satellite to estimate the effect under consideration [18]. It is one of the most suitable satellites: it has a very high orbit and a very large eccentricity, and it is these parameters that make the main contribution to the studied effect. Nevertheless, no detailed calculations have been carried out, whereas a comprehensive study of the effect of pulse deviation as a result of relativistic corrections by examples of various real-world ESS is a very important task.

We have conducted such a study with several RadioAstron ESS [18] and all 24 ESS of the GLONASS constellation [19]. For this purpose, a proprietary algorithm for numerical calculation was developed within the framework of both methods. Since they differ by no more than thousandths of a second, we present unified results. The software consists of two components: a graphical interface for setting the calculation parameters and a library of data calculations by parameters. The output of graphs according to the specified parameters is implemented. The following values are used: for the parameters of the Earth: $R_\oplus = 6.378137 \times 10^6$ m, $\Omega = 7.292211\times10^{-5}\times s^{-1}$, $GM_\oplus = 3.98603\times10^{14} m^3\times s^{-2}$; for the speed of light: $s = 299.792458\times10^6$ m$\times s^{-1}$. The effect was calculated both for the actual parameters of the ESS orbits and for their variations.

First of all, calculations were made for the RadioAstron satellite to verify theoretical formulae and numerical programs. In fact, the formulae were applied to real satellites, but it is not known how close the obtained estimate is to the real effect. In a certain sense, it is a simulated model in which the effect and its properties are most pronounced. The data from [18] were used for calculations, and the following parameters were selected: $a(1+e) = 3.5 \times 10^5$ km, $a(1-e) = 5.0 \times 10^4$ km, $i = 51.6°$, $\omega = 0°$, $\lambda = 0°$, $\varphi_0 = 56°00'$, $\lambda_0 = 36°49'$.

Changes in the angle α over the orbital period are shown in Fig. 1. At its maximum, the effect has a significant value, but not exceeding 36″. The effect observed from the selected station is indicated in gray, where the limitation is the position at 15° above the horizon.

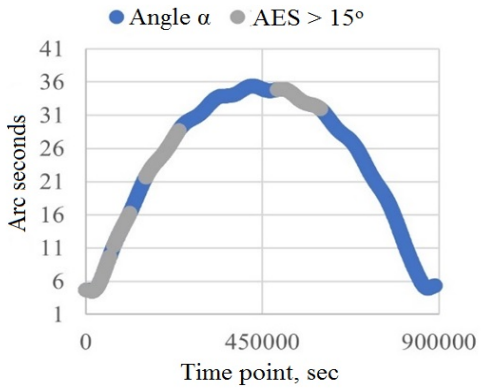

Fig. 1. Change in α during the orbital period of the RadioAstron ESS.

The parameters of the RadioAstron satellite orbit change approximately every 5 years [18]. These data were decrypted to obtain the parameters of the satellite's orbit over 5 years from December 2017. Angle was calculated for each of the days of the cycle at the beginning of the day, and its change over the 5-year cycle is shown in Fig. 2. The maximum effect value for the data [18] is about 16″. The maximum value of 36″ was not obtained, because the effect was calculated

only at the beginning of the day without reference to the maximum.

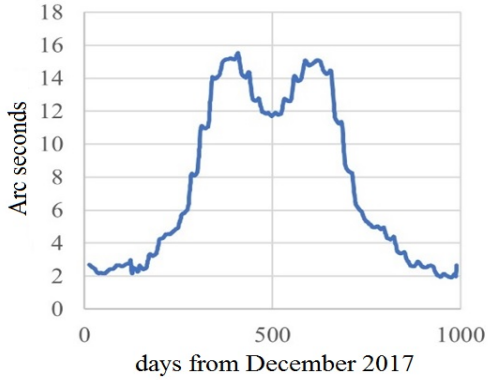

Fig. 2. Changes in α for the RadioAstron ESS over 5 years.

To assess how significantly and qualitatively the effect depends on the parameters, calculations were made for the initial data set with variations in the angle of inclination i, the longitude of the ascending node λ, the perigee argument ω, and the eccentricity e. It turned out that the changes in i and λ do not significantly affect the range of angle changes over the orbital period. The reason is that such variations do not change the distance to the satellite much (no graphs are provided here), while the variations of ω and e (see Figs. 3 and 4) do change this distance, and therefore the effect, significantly. For example, for $e = 0.9$, the effect reaches 44″. The large value of the initial eccentricity is important for these results.

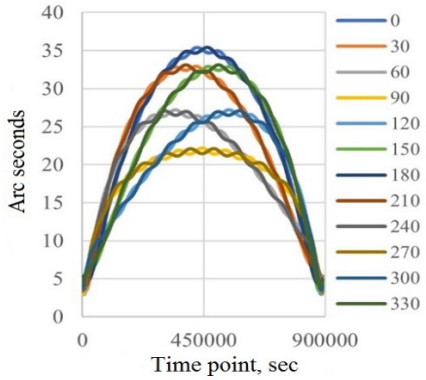

Fig. 3. Changes in α during the orbital period of the RadioAstron satellite for different values of the perigee argument ω from 0° to 330° in increments of 30°

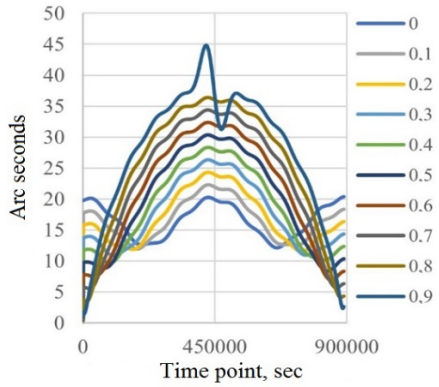

Fig. 4. Changes in α during the orbital period of the RadioAstron satellite for different values of eccentricity e from 0 to 0.9 in increments of 0.1.

The calculations to determine the effect of signal deviation for GLONASS constellation were made using the data from [19]:

NS	Date	T	e	i	λ	ω
1	07.08.2023	40544.7	0.00032	64.49517	50.36562	13.68347
2	07.08.2023	40544.24	0.00197	64.93737	30.58079	–132.336
3	07.08.2023	40544.24	0.00192	64.77635	178.5927	–127.573
4	07.08.2023	40544.2	0.00095	65.08466	158.6894	–103.557
5	07.08.2023	40544.17	0.00054	65.09873	138.5206	–146.146
6	07.08.2023	40544.28	0.00059	64.47887	111.6534	128.3038
7	07.08.2023	40544.27	0.00165	64.78391	92.95447	–127.447
8	07.08.2023	40544.2	0.00207	64.79112	73.44463	–107.474
9	07.08.2023	40543.94	0.00185	63.62056	177.468	–154.111
10	07.08.2023	40543.76	0.00158	64.32575	159.6166	0.714111
11	07.08.2023	40543.79	0.00064	64.59576	–52.5411	–122.261
12	07.08.2023	40543.95	0.00115	64.36848	–75.1393	–75.5475
13	07.08.2023	40543.73	0.00025	64.31682	–94.8321	85.95703
14	07.08.2023	40543.9	0.00078	64.08078	–117.771	–122.695
15	07.08.2023	40543.91	0.00092	64.29604	–138.274	–98.1189
16	05.08.2023	40544	0.00092	64.73361	157.7343	–141.817
17	05.08.2023	40544.16	0.00096	65.52239	73.30216	–171.639
18	05.08.2023	40544.09	0.001	65.78624	54.10217	–22.4396
19	05.08.2023	40543.93	0.00025	66.03824	37.67246	139.4495
20	05.08.2023	40544.1	0.00075	66.05248	12.93022	–9.87122
21	05.08.2023	40543.55	0.00067	65.72478	–12.3852	167.4426
22	05.08.2023	40544.13	0.00085	64.77618	–29.8859	–75.3442
23	05.08.2023	40543.5	0.00041	65.90193	–53.3656	96.5863
24	05.08.2023	40544.07	0.00062	64.86202	–74.5611	–134.467

Note: $T = 2\pi\sqrt{a^3/GM_\oplus}$ is the orbital period in seconds.

Mendeleevo-1 station with coordinates $\varphi_0 = 56.0267°$, $\lambda_0 = 37.2234°$ was chosen to be the laser station. The effect was calculated for all satellites. As expected, the main contribution to it is made by the satellite distance from the origin of the topocentric frame. All GLONASS satellites differ little from each other in terms of the orbit shape, therefore, for a more detailed study, two satellites with the maximum major semi-axis and the minimum major semi–axis were taken: GLONASS-1 and GLONASS-23. The results of their study are discussed in the article. Figures 5 and 6 show the graphs of the effect for each of these satellites during their orbital periods. In both cases, the maximum value of the effect is about 2.9". It should be noted that the difference between the maximum values of the effect for each of them is only about 0.2", which is insignificant, but generally can be detected.

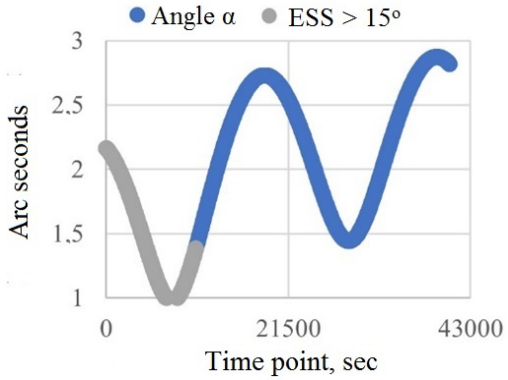

Fig. 5. Change in angle α during the orbital period of GLONASS-1 ESS.

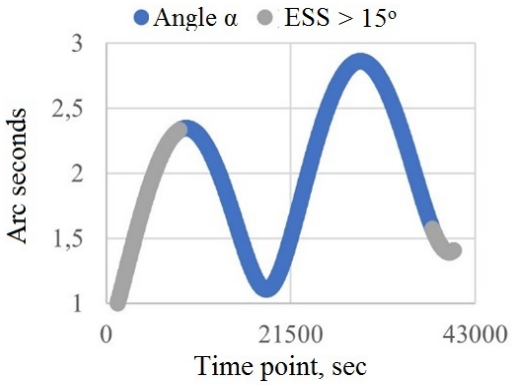

Fig. 6. Change in angle α during the orbital period of GLONASS-23 ESS.

Calculations were made with variations in the data set of each of these two satellites. The results of variations in the angle of inclination i for GLONASS-1 satellite are shown in Fig. 7, in the ascending node longitude λ—in Fig. 8, in the perigee argument ω—in Fig. 9, and in the eccentricity—in Fig. 10.

The results of variations differ qualitatively from those for RadioAstron satellite (significantly different scales should be taken into account). The reason for the differences is considerably lower value of the major semi–axis and the extremely small eccentricity; however, the main dependence of the pulse deviation effect on distance remains.

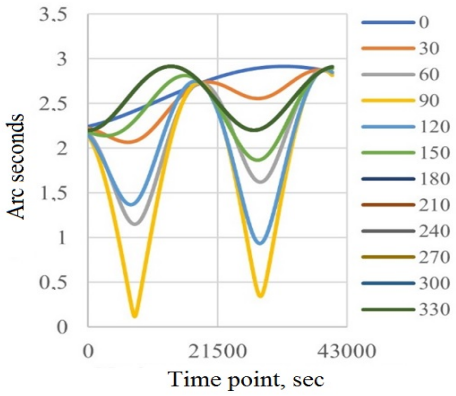

Fig. 7. Changes in α during the orbital period of GLONASS-1 ESS at different angles of the orbit inclination i from 0° to 330° in increments of 30°.

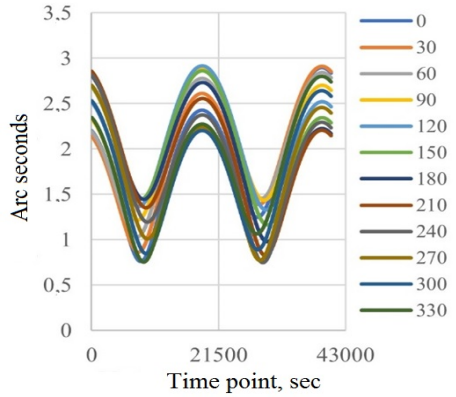

Fig. 8. Changes in α during the orbital period of GLONASS-1 ESS at different longitudes of the ascending node λ from 0° to 330° in increments of 30°.

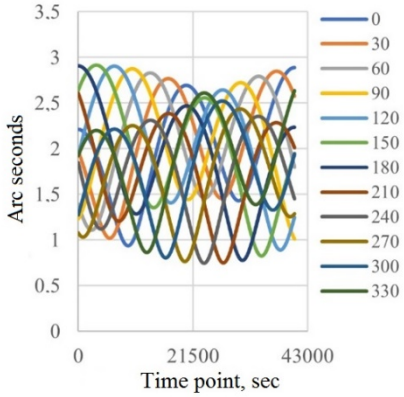

Fig. 9. Changes in α during the orbital period of GLONASS-1 ESS at different values of the perigee argument ω from 0° to 330° in increments of 30°.

Research prospects. The considered model does not fully correspond to reality. The development of the model and the estimation of factors that have not been taken into account so far seem to be essential. There are at least two of them: non-sphericity of the Earth, which

will affect the ESS coordinates (4) in the reference system of the station, and the Newtonian potential of the Earth, the value of which is comparable to the centrifugal potential at the height of the orbits. The results should be compared with the results of [12]. For the purposes of the study, the values of gravitational potential will be entered in (1).

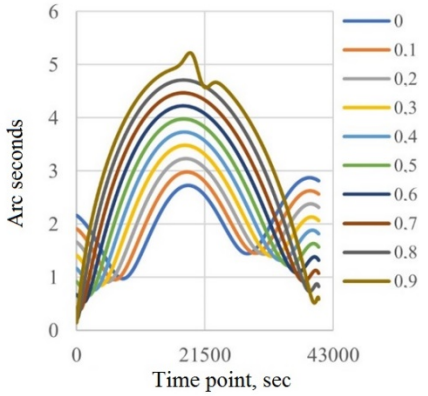

Fig. 10. Changes in α during the orbital period of GLONASS-1 ESS at different eccentricities *e* from 0 to 0.9 in increments of 0.1.

The numerical calculations showed that in the case of GLONASS satellites, their small eccentricities do not make a significant contribution in the effect, so the calculations for them can be simplified by neglecting both the eccentricities and the perigee arguments. This simplification provides a real opportunity to create a program for determining the variations in orbit parameters by analyzing the variations in of pulse deviation effect. Further, such a program can be generalized for ESS with arbitrary parameters.

CONCLUSIONS

The paper presents the calculations of relativistic effect of electromagnetic pulse deviation during laser ranging of an ESS, which have been combined and compared to the results of [13] and [15]. The ESS coordinates in its Keplerian orbit are determined at each time point, and the equations of laser signals propagation are given. By calculating the direction of tangents to the trajectories of emitted and returned signals, the angle between them is determined. Estimations are made for acceptable approximations. Theoretical calculations are carried out in various ways: by normalizing them at the moment of signal reflection from satellite, or by normalizing the final formulae at the moments of reflected signal emission and reception. In a theoretical sense, these approaches are equivalent, although the normalization at the time of reflection (19) describes the effect as an explicit function of the satellite's position in orbit.

The formulae were used to numerically calculate the effect for real ESS, such as RadioAstron [16] and all 24 ESS of the GLONASS constellation [17]. In the future, it is planned to estimate the influence of weaker factors, in particular, the Earth's gravity field and ellipticity. Taking into account the magnitude of the laser pulse deviation caused by relativistic laws, it is possible to improve the ESS positioning. Detection of the deviation effect can be used both for fixing the parameters of satellite orbits, including their abnormal variations, and for testing the relativistic theory (not only SR or GR, but also generalized theories of gravity).

FUNDING

The study was carried out within the framework of the Federal Program of GLONASS Sustainment, Development and Use under the state program of the Russian Federation "Space Activities of Russia" for 2021–2030, registration number 1210806000081-5 in the Integrated National Information System EGISU.

CONFLICT OF INTEREST

The authors of this work declare that they have no conflicts of interest.

REFERENCES

1. Chaplinskii, V.S., Application of relativistic theory to spacecraft trajectory measurements, *Kosmicheskie issledovaniya*, 1985, vol. 23, no. 1, pp. 49–62.
2. Brumberg, V.A., Relyativistskaya nebesnaya mekhanika (Relativistic Celestial Mechanics), Moscow: Nauka, 1972.
3. Bartels, N., Allenspacher, P., Hampf, D. et al., Space object identification via polarimetric satellite laser ranging, *Communications Engineering*, 2022, vol. 1, p. 5. https://doi.org/10.1038/s44172-022-00003-w
4. EUROLAS Data Center, https://edc.dgfi.tum.de/en/.
5. Glaser, S., König, R., Neumayer, K. et al., Future SLR station networks in the framework of simulated multi-technique terrestrial reference frames, *Journal of Geodesy*, 2019, vol. 93, pp. 2275–2291. https://doi.org/10.1007/s00190-019-01256-8
6. Hampf, D., Schafer, E., Sproll, F. et al., Satellite laser ranging at 100 kHz pulse repetition rate, *CEAS Space Journal*, 2019, vol. 11, pp. 363–370. https://doi.org/10.1007/s12567-019-00247-x
7. Wilkinson, M., Schreiber, U., Procházka, I. et al., The next generation of satellite laser ranging systems, *Journal of Geodesy*, 2019, vol. 93, pp. 2227–2247. https://doi.org/10.1007/s00190-018-1196-1
8. Xue, L., Li, Z., Zhang, L. et al., Satellite laser ranging using superconducting nanowire single-photon detectors at 1064 nm wavelength, *Optics Letters*, 2016, vol. 16, pp. 3848–3851. https://doi.org/10.1364/OL.41.003848
9. Kucharski, D., Kirchner, G., Otsubo, T., and Koidl, F., A method to calculate zero-signature satellite laser ranging

normal points for millimeter geodesy – a case study with Ajisai, Earth, Planets and Space, 2015, vol. 67, article no. 34. https://doi.org/10.1186/s40623-015-0204-4
10. Ashby, N., Relativity in the Global Positioning System, *Living Reviews in Relativity*, 2003, vol. 6, pp. 1–42. https://doi.org/10.12942/lrr-2003-1
11. Denisov, M.M., Kravtsov, N.V., and Krivchenkov, I.V., Optical effects in a rotating frame of reference, *JETP Letters*, 2007, vol. 85, no. 8, pp. 412-414 https://doi.org/10.1134/S0021364007080140
12. Denisov, M.M., Relativistic corrections in the laser ranging of spacecraft, *Mathematical Models and Computer Simulations*, 2009, vol. 1, no.3, pp. 393-401. https://doi.org/10.1134/S2070048209030065
13. Denisov, V.I. and Denisov, M.M., Mathematical modeling of angular distortions in laser ranging of the RadioAstron satellite, *Computational Mathematics and Mathematical Physics*, 2008, vol. 48, no. 8, pp. 1418–1427. https://doi.org/10.1134/S0965542508080113
14. Denisov, M.M. and Zubrilo, A.A., Study of laser beam propagation in a rotating reference frame, *Moscow University Physics Bulletin*, 2009, no. 6, pp. 569–572.
15. Ostanina, M.V., Pasisnichenko, M.A.,and Rostovskii, V.S., Mathematical modeling of relativistic effect in laser ranging of artificial Earth satellites, *Moscow University Physics Bulletin*, 2013, no. 6, pp. 42–46. https://doi.org/10.3103/S0027134909060022
16. Mazaeva, I.V. and Pasisnichenko, M.A., The effect of the relativistic transformation law of angles on laser ranging of satellites moving in circular orbits equipped with a single retroreflector, *Moscow University Physics Bulletin*, 2017, no. 4, pp. 402–409. https://doi.org/10.3103/S0027134917040087
17. Mazaeva, I.V., Gavrish, O.N., and Lebedeva, M.V., A numerical study of laser ranging efficiency of artificial Earth satellites in elliptical orbits, *Moscow University Physics Bulletin*, 2021, no. 4, pp. 240–245. https://doi.org/10.3103/S002713492104007X
18. RadioAstron User Handbook, prepared by the RadioAstron Science and Technical Operations Group, Version 2.94, 10 December 2019.
19. GLONASS data: https://glonass-iac.ru/glonass/ephemeris/
20. Landau, L.D. and Lifshits, E.M., *Teoriya polya* (Field Theory), Moscow: Nauka, 1988.
21. Montenbruck, O. and Gill, E., Satellite orbits: Models, Methods, and Applications, Springer: Heidelberg, Dordrecht, London, New York, 2012. https://doi.org/10.1007/978-3-642-58351-3